Antibody to Granulocyte Macrophage Colony–stimulating Factor Reduces the Number of Activated Tissue Macrophages and Improves Left Ventricular Function After Myocardial Infarction in a Rat Coronary Artery Ligation Model

Robert S. Kellar, PhD, Jordan J. Lancaster, BS,† Hoang M. Thai, MD,† Elizabeth Juneman, MD,† Nicholle M. Johnson, BS,† Howard G. Byrne,† Maribeth Stansifer, BS,† Reza Arsanjani, MD,† Mark Baer, PhD,‡ Christopher Bebbington, PhD,‡ Michael Flashner, PhD,‡ Geoffrey Yarranton, PhD,‡ and Steven Goldman, MD†*

Abstract: Granulocyte macrophage colony–stimulating factor (GM–CSF) promotes infarct expansion and inappropriate collagen synthesis in a myocardial infarction (MI). This study was designed to determine if treatment with anti-GM–CSF will inhibit macrophage migration, preserve function, and limit left ventricular (LV) remodeling in the rat coronary artery ligation model. Treatment with a monoclonal antibody to GM–CSF (5 mg/kg) was initiated 24 hours before coronary artery ligation and continued every 3 days for 3 weeks. Left coronary arteries of rats were ligated, animals were recovered, and cardiac function was evaluated 3 weeks postligation. Tissue samples were processed for histochemistry. Anti-GM–CSF treatment increased LV ejection fraction (37 ± 3% vs 47 ± 5%) and decreased LV end systolic diameter (0.75 ± 0.12 vs 0.59 ± 0.05 cm) with no changes in LV systolic pressure (109 ± 4 vs 104 ± 5 mm Hg), LV end diastolic pressure (22 ± 4 vs 21 ± 2 mm Hg), LV end diastolic diameter (0.96 ± 0.04 vs 0.92 ± 0.05 cm), or the time constant of LV relaxation tau (25.4 ± +2.4 vs 22.7 ± 1.4 milliseconds) ($P < 0.05$). Significantly lower numbers of tissue macrophages and significant reductions in infarct size were found in the myocardium of antibody-treated animals (81 ± 21.24 vs 195 ± 31.7 positive cells per 0.105 mm^2, compared with controls. These findings suggest that inhibition of macrophage migration may be beneficial in the treatment of heart failure after MI.

Key Words: granulocyte macrophage colony–stimulating factor, GM–CSF, antibody, activated macrophages, myocardial infarction, left ventricular function

(*J Cardiovasc Pharmacol*™ 2011;57:568–574)

Received for publication October 4, 2010; accepted January 30, 2011.

From the *Development Engineering Sciences, LLC, Flagstaff, AZ; †Southern Arizona VA Health Care System, Sarver Heart Center, University of Arizona, Tucson, AZ; and ‡Kalobios, South San Francisco, CA.

The authors declare no conflicts of interest.

Reprints: Robert S. Kellar, PhD, 708 N. Fox Hill Rd, Flagstaff, AZ, 86004 (e-mail: rskellar@des-company.com).

INTRODUCTION

Heart failure is a leading cause of morbidity and mortality in developed nations.[1] Left ventricular (LV) remodeling is the alteration of myocardial structure and function that occurs after myocardial infarction (MI) and results in progression to heart failure. The LV remodeling after MI is associated with structural changes involving extracellular matrix,[2,3] fibrosis,[4] cellular damage,[5] and cell death.[6,7] This ultimately leads to LV dilatation, thinning, and scarring of the infarcted myocardium and compensatory hypertrophy of noninfarcted myocardium.[8] Although the exact role of inflammation in LV remodeling and heart failure is not well understood, inflammatory cytokine levels are elevated in heart failure and become more prominent with a concomitant decline in myocardial function.[9–12] Peripheral monocytosis is associated with LV dysfunction[13] after MI and is one of several important independent predictors of the progression to heart failure in survivors of MI.[14] Mononuclear cells (monocytes and macrophages) are integral to the infarct and wound healing process through a cascade of events that involve matrix turnover, growth factors, and cytokines.

Granulocyte macrophage colony–stimulating factor (GM–CSF) is one of a family of cytokines/growth factors that has a potent effect in upregulation, proliferation, and maturation of monocytes and macrophages.[15] GM–CSF induces peripheral monocytosis, upregulates monocyte chemoattractant protein-1 (MCP-1) levels,[16] and plays an important role in monocyte transendothelial migration.[17] GM–CSF and its receptor levels are elevated in patients with advanced dilated cardiomyopathy.[18,19] In addition, GM–CSF has been shown to facilitate postinfarct expansion and heighten early postinfarction LV remodeling in the rat.[20,21] The aim of this study was to determine the role of GM–CSF in the progression to heart failure after acute MI by blocking its activity with a specific anti-GM–CSF antibody.

MATERIALS AND METHODS

Mab518 Anti-Granulocyte Macrophage Colony–stimulating Factor Monoclonal Antibody

Murine antirat GM–CSF monoclonal antibody 83329 was obtained from R&D Systems (MAB518, R&D Systems, Minneapolis, MN). The antibody neutralizes the activity of rat GM–CSF in a murine DA-3 cell proliferation assay (50% inhibitory concentration value [IC_{50}] < 0.8 μg/mL for neutralization of 0.5 ng/mL rat GM–CSF).

Experimental Design

Normal adult male Sprague–Dawley rats (8–10 weeks old; Harlan, Indianapolis, IN) were enrolled in the study after being assigned random study numbers and were selected in a random and blinded fashion for treatment and evaluation. Rats were randomized into 3 groups: sham surgery, MI with saline control, or treatment with anti-GM–CSF (5 mg/kg, MAB518) 24 hours before MI and 5 mg/kg 3 times per week for 3 weeks, delivered intraperitoneally. End points were measured at 3 weeks after MI. The experiments were performed in an American Association for Accreditation of Laboratory Animal Care–accredited facility with approval from the animal use committees of the Southern Arizona Veterans Affairs Health Care System and the University of Arizona (Tucson, AZ).

Detection of Mab518 Anti-Granulocyte Macrophage Colony–stimulating Factor Monoclonal Antibody in Serum

Enzyme-linked immunosorbent assay plates (Costar, Corning, Inc, Lowell, MA) were coated with recombinant rat GM–CSF at 50 ng per well in 50 μL phosphate buffered saline (PBS) for 1 hour at 37°C and blocked with 5% powdered skimmed milk (Marvel, Premier Foods, St Albans, Hertfordshire, United Kingdom) in PBS, Tween-20 (PBST) for 1 hour at 37°C. Serial dilutions of serum samples were added to the plates for 1 hour and compared to Mab518 standard, starting at 500 μg/mL. Wells were washed 3 times with PBST and polyclonal goat antimouse IgG-HRP (1:2000 in PBST, Dako, Carpinteria, CA) was added at 50 μL per well for 45 minutes at room temperature, wells were washed 3 times with PBST, once with PBS, and 100 μL of 3,3′,5,5′ tetramethyl benzidine (TMC reagent) (Sigma, St. Louis, MO) added. Reactions were stopped with 100 μL of 2M $H2SO_4$, and the absorbance at 450 nm was measured. Data were analyzed by Prism 5.0 software and concentrations calculated by comparison to the antirat GM–CSF standard curve.

Myocardial Infarction Model

Heart failure was created in rats using standard published techniques from our laboratory.[22–24] In brief, rats were anesthetized with ketamine and acepromazine and a left thoracotomy performed. The heart was expressed from the thorax and a ligature placed around the proximal left coronary artery. The heart was returned to the chest and the thorax closed. The rats were maintained on standard rat chow, water ad libitum and pain medication postoperatively. Infarcted rats undergoing this procedure have large MIs averaging 40% of the ventricle.[25,26] The lungs were inflated, the chest closed, and the rat allowed to recover. Sham surgery animals were anesthetized, left thoracotomy performed, but litigation of the proximal left coronary artery did not occur.

Hemodynamics

Hemodynamics were measured using previously published methods from our laboratory.[22–24,26] In brief, rats were anesthetized with inactin (100 mg/kg intraperitoneal injection) and placed on a specially equipped operating table with a heating pad to maintain constant body temperature. After endotracheal intubation and placement on a rodent ventilator, a 2F solid state micromanometer tipped catheter with 2 pressure sensors (Millar, Houston, TX) was inserted via the right femoral artery, with one sensor located in the LV and another in the ascending aorta. The pressure sensor was equilibrated in 37°C saline before obtaining baseline pressure measurements. After a period of stabilization, LV and aortic pressures, and heart rate were recorded and digitized at a rate of 1000 Hz using a PC equipped with an analog–digital converter and customized software. From these data, LV dP/dt and the time constant of LV relaxation (tau) were calculated.

Echocardiography

Open-chest intrathoracic echocardiography was obtained at baseline and 3 weeks after coronary artery ligation. A Vingmed, Vivid 7 System (GE Ultrasound, Waukeasha, WI) echo machine was used equipped with EchoPac programming software and a 10-MHz transducer with views obtained in the parasternal short-axis view. These images were digitized in sequential frames for 2-dimensional and M-mode measurements of LV dimensions throughout the cardiac cycle. The anterior wall was noted as the infarcted segment; the posterior wall was noted as the noninfarcted segment.

Left Ventricular Ejection Fraction

Linear measurements to determine LV performance such as ejection fraction (EF) were obtained by M-mode in the short-axis view. Cursor placement was performed in diastole and systole through the interventricular septum, the internal dimensions of the LV, and the posterior wall in its minor axis.

Left Ventricular Pressure–Volume Relationships

LV pressure–volume relations were measured as previously described from our laboratory.[25,27] In brief, at the end of the study, the heart was arrested with potassium chloride, and a catheter consisting of PE-90 tubing with telescoped PE-10 tubing inside was inserted into the LV via the aortic root. One end of the double-lumen LV catheter was connected to a volume infusion pump (Harvard Apparatus, Holliston, MA), whereas the other end was connected to a pressure transducer zeroed at the level of the heart. The right ventricle was partially incised to prevent loading on the LV. The LV was filled (1.0 mL/min) to 60–100 mm Hg and unfilled while pressure was recorded onto a physiologic recorder (Gould Instruments, Valley View, OH); ischemic time was limited to 10 minutes, the volume infused was a function of filling rate.

Histochemistry

After hemodynamic measurements, formaldehyde fixed tissue samples from both treatment groups (antibody treated and untreated, saline controls) were processed for histochemical evaluation using markers specific for activated tissue macrophages (CD68) and microvasculature elements (*Griffonia simplicifolia* lectin). These samples were subsequently evaluated using quantitative morphometry to report the number of activated tissue macrophages per unit area and the number of microvascular profiles per unit area.

Fixed tissue samples were dehydrated, brought to paraffin, and block embedded. Sections (6 μm) were subsequently processed for histochemical evaluation. These sections were reacted with anti-CD68 antibody, a marker for activated monocytes and macrophages (Serotec, clone ED1, Raleigh, NC) used at a final dilution of 1:100. Primary antibody was visualized using a secondary antibody with a peroxidase reaction product recognition system (Universal mouse kit; Dako, Inc., Carpinteria, CA). Separate sections were evaluated using the *Griffonia. simplicifolia* lectin to identify vascular elements (peroxidase conjugated lectin-Gs-1; EY Laboratories, San Mateo, CA used at a final concentration of 1:100). The Gs-1 lectin binding was visualized using a peroxidase reaction product. For both histochemical techniques (CD68 and Gs-1), a methyl green counter stain was used to identify background nuclei.

Microvessel Density/Inflammatory Cell Density

Variability in the size and extent of the infarct in the current model is known to result in hearts that have various degrees of myocardial damage. This variability could influence quantitative results. Therefore, sections from each treatment group (antibody treated and untreated saline controls) were first grossly selected for an obvious thinned myocardial wall that represents significant myocardial damage. In this way, all sections evaluated had similar degrees of resulting myocardial damage. Next, sections were blind coded and randomized for subsequent quantitative morphometry evaluation.

For microvessel density counts, the number of cross sectional and longitudinal blood vessel profiles per high powered field (HPF = 0.105 mm^2 using a ×25 objective) were counted. Three random HPF counts were taken within the thinned myocardium (n = 3 per group). The criteria for the positive count of a vessel were (1) positive Gs-1 reaction, (2) an identifiable lumen, and (3) within the designated high magnification. A micrometer was used to calibrate each image. Each image was individually imported into an Image Analysis Software Program (Image J 1.39u, National Institutes of Health, USA), calibrated, and then evaluated for microvessel density counts. A 2-tailed Student's *t*-test was used for statistical comparisons.

For inflammatory cell density counts, the numbers of CD68 positive reacting cells were quantified using the same above procedures where 3 random HPF counts were taken within the thinned myocardium (n = 5 per group). A 2-tailed Student's *t*-test was also used for statistical comparisons.

Infarct Area and Percent Infarct Measurements

For infarct area and percent infarct measurements, trichrome-stained cross sections were digitally scanned using the Aperio ScanScope CS whole-slide digital scanner (n = 5 per group). Measurements and calculations were collected on each whole-slide digital scan using the ImageScope Software v10.0.36.1808. A 2-tailed Student's *t*-test was used for statistical comparisons.

Statistics

Data were expressed as mean ± standard error (SE). For the physiologic and echocardiographic measurements, Student's *t*-test was used for single comparison of Sham versus other study groups. Interactions were tested using 2-way analysis of variance, intergroup differences were evaluated using the Student–Newman–Keuls test for statisticalsignificance. Pressure–volume relations were evaluated using multiple linear and polynominal regression analysis. The correlation of statistical difference was based on the Durbin–Watson statistic, F-statistic, *P* value ($P < 0.05$), and variance coefficients.

RESULTS

Study Mortality Rates

Mortality rates in this study were 42% and 46% in untreated control animals and in anti-GM–CSF-treated animals, respectively.

Echocardiographic Changes in Left Ventricular Function and Dimensions

The data on global LV function and dimension are shown in Figures 1–3. Figure 1 illustrates that anti-GM–CSF-treated animals had a significant increase in LV EF compared with untreated animals. These EF values were not returned to control Sham surgery levels; however, they were significantly higher compared with those of untreated animals that fell below the 40% EF value, which indicates that these animals had progressive heart failure. Figure 2 shows that the LV end systolic diameter in anti-GM–CSF-treated animals was statistically lower compared with untreated controls; this finding is consistent with the differences in LV EF (Fig. 1) and again supports the observation that untreated control animals had worsened in condition, more consistent with a heart failure etiology. No difference in LV end diastolic diameter (Table 1) was detected. These data suggest that the primary mode of action of the antibody therapy influences systolic events in the cardiac cycle.

In Vivo Hemodynamics

No changes in LV systolic pressure or LV end diastolic pressure in anti-GM–CSF-treated animals and untreated control animals were found (Table 1). This indicates that there is no afterload reduction resulting from the anti-GM–CSF. Table 1 also reports no change in the time constant of LV relaxation tau. This suggests that there is no change in the relaxation component of diastolic function.

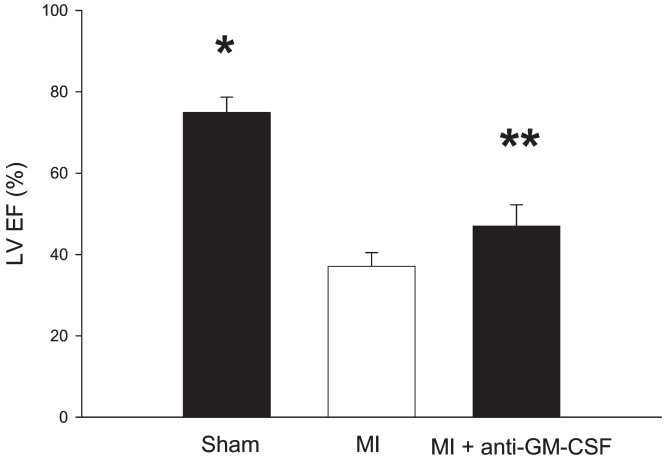

FIGURE 1. LV EF (%) among treated groups. Sham (n = 5), MI (n = 10), MI + anti-GM–CSF (n = 12). Data are mean ± SE. *$P < 0.05$ versus MI and MI + anti-GM–CSF. **$P < 0.05$ versus MI and Sham.

Detection of Mab518 Anti-Granulocyte Macrophage Colony–stimulating Factor Monoclonal Antibody in Serum

Rat sera were collected 1 day after the last administration of antibody, and the concentration of Mab518 in the serum was determined using a GM–CSF-binding enzyme-linked immunosorbent assay. All animals had detectable levels of Mab518 in the serum at this time point (9.2 μg/mL to >1 mg/mL, median = 272 μg/mL), indicating that functional anti-GM–CSF antibody was maintained throughout the course of the study in all animals.

Histochemistry and Morphometry

Evaluation of the Gs-1 lectin-reacted sections did not demonstrate any differences between the 2 treatment groups. These data suggest that the anti-GM–CSF treatment did not affect microvessel density.

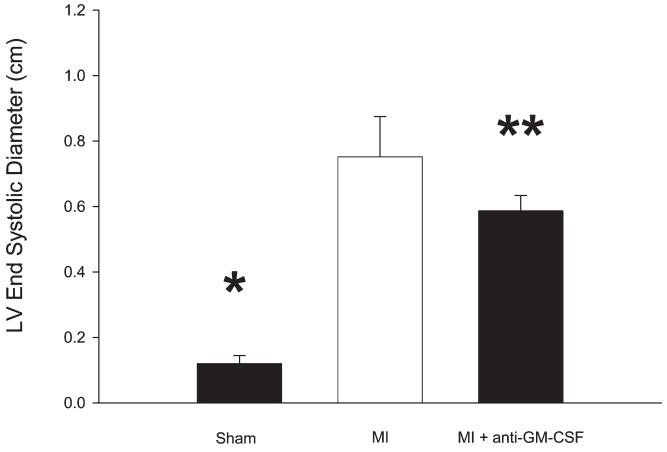

FIGURE 2. LV end systolic diameter (cm) for Sham, MI and MI + anti-GM–CSF. Sham (n = 4), MI (n = 5), MI + anti-GM–CSF (n = 9). Data are mean ± SE. *$P < 0.05$ versus MI + anti-GM–CSF. **$P < 0.05$ versus MI.

Hearts from rats treated with anti-GM–CSF demonstrated statistically fewer activated tissue macrophages in the region of the damaged myocardium compared with saline control animals (Fig. 3). Additionally, these results are supported by quantitative morphometry data from immunohistochemistry analysis using anti-CD68 antibody. These results demonstrate statistically lower numbers of activated tissue macrophages in infarcted myocardium of antibody-treated animals compared with saline controls (81 ± 21.24 CD68 vs 195 ± 31.7 positive cells per 0.105 mm^2, respectively) (Fig. 4).

Infarct Area and Percent Infarct

Representative trichrome-stained sections of LV cross sections from saline control and anti-GM–CSF-treated hearts illustrate structural differences between the 2 treatment conditions (Fig. 5). Subsequent morphometry analysis using whole-slide digital scans revealed significantly larger infarct areas in saline-treated animals compared to anti-GM–CSF-treated hearts (10.48 ± 2.69 mm^2 vs 6.01 ± 2.58, respectively, $P < 0.02$). Additionally, the percent infarct area was statistically lower in anti-GM–CSF-treated hearts (16.39 ± 8.53% vs 34.76 ± 5.76%, $P < 0.01$, Fig. 6).

DISCUSSION

In this study, we report improvement in LV EF and an improvement in LV end systolic diameter in animals that received an antibody that neutralizes GM–CSF. Additionally, these treated animals had a decrease in the number of activated tissue macrophages, a reduction in infarct size and the percent of infarct area thus suggesting a more favorable outcome of LV remodeling after infarction. Finally, we report a reduction in the number of treated animals that progress to heart failure in animals treated with an antibody that neutralizes GM–CSF. The exact mechanism of this antibody mediated improvement in global LV function and reduction of LV remodeling is unknown; however, several mechanisms could be involved. As mentioned previously, LV remodeling after MI is the result of multiple processes including local ischemia leading to cellular damage and death,[5–7] oxidative stress,[28] changes in extracellular matrix,[2,3] and fibrosis.[4] MI is associated with the inflammatory process, which is necessary for healing and scar formation.[29,30] This inflammatory process is one of the mechanisms that eventually leads to LV remodeling and progression of heart failure. Mononuclear cells play an integral role in this healing process. Previous studies have shown an association between peripheral monocytosis and worsening LV dysfunction with progression of heart failure.[13,14] GM–CSF is a potent stimulator of monocytes and leads to peripheral monocytosis[15] and delays macrophage and monocyte apoptosis resulting in more persistent inflammation in the infarcted myocardium.[31,32]

Previously, Tanimoto et al[16] demonstrated that MCP-1 expression is enhanced by GM–CSF. MCP-1 is involved in the healing response after an acute coronary event,[33] and MCP-1 expression is markedly but transiently elevated after MI.[34–36] In addition, absence of MCP-1 leads to suppression of the inflammatory response and results in attenuated remodeling of the infarcted ventricle.[37,38] Therefore, it is possible that treatment with anti-GM–CSF results in reduction in MCP-1

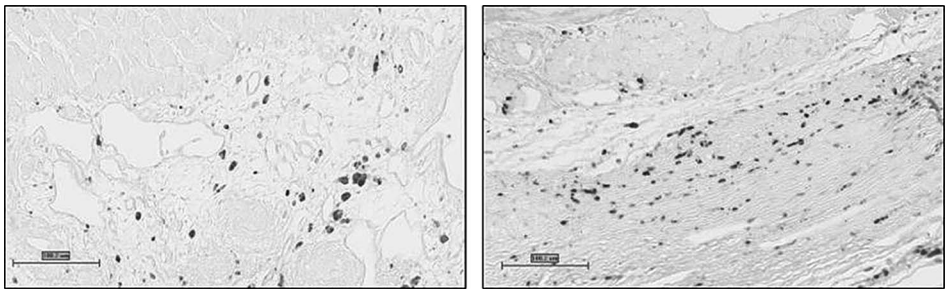

FIGURE 3. Representative immunohistochemistry results from CD68 antibody (activated macrophages) for anti-GM–CSF–treated heart (left) and NaCl-treated heart (right). Scale bars = 100 μm.

level. The lower MCP-1 levels would then lead to an overall decline in the inflammatory process and attenuate deleterious LV remodeling.

In other studies, neutralizing monoclonal antibodies have been used to inhibit neutrophil accumulation within the myocardium of an acute myocardial reperfusion injury model in canines.[39,40] These studies help to validate the concept of utilizing a blocking antibody to inhibit specific inflammatory pathways that contribute to deleterious myocardial remodeling after a cardiac event. In one study, the mean size of the myocardial infarct was significantly reduced in anti-Mo1-treated animals[39] with no effect on regional blood flow. However, these studies did not report long-term cardiac function results due to the acute nature of the model.

Collagen synthesis and degradation play an important role in cardiac remodeling. Fibroblasts are stimulated after MI and cause fibrosis of both infarcted and noninfarcted regions of the ventricle.[2–4] Collagen turnover is enhanced after MI and increased collagen deposition at the site of myocyte necrosis play an essential role in preserving LV structure and function.[41,42] Excessive collagen degradation and impaired fibrosis may lead to enhanced infarct expansion.[43,44] The administration of romurtide, which is a potent GM–CSF inducer, leads to inhibition of collagen production in the infarcted region.[21] It could be probable that romurtide at lower concentrations may be cardioprotective or that anti-GM–CSF may exert the beneficial functional effect through some other mechanism.

Extracellular matrix is degraded by matrix metalloproteinases (MMP), which are markedly overexpressed after MI. The increase in MMP-1 expression and collagen degradation has been shown to be directly correlated with end diastolic volume and inversely correlated with LV function.[43] In addition, MMP-9 knockout mice or those treated with MMP inhibitor have been shown to have less LV dilatation after MI.[45,46] GM–CSF has been reported to enhance expression of MMP-1, MMP-9, and MMP-12.[47,48] Collagen content was lower after MI in romurtide (GM–CSF inducer) treated rats than controls, hypothesizing that excessive infiltration of inflammatory cells may result in imbalance of extracellular matrix synthesis/degradation resulting in adverse LV remodeling.[21] Therefore, binding of GM–CSF might lead to decreased expression of MMP and less LV dilatation after MI. This proposed mechanism may in part explain the clinical side effects seen with GM–CSF subcutaneous delivery in patients. GM–CSF has been used as a prophylactic therapy of infection in immunosuppressed patients.[49] The drug has been described to have several side effects,[50] including deleterious effects on cardiac function, specifically LV end diastolic diameter measurements, cardiac output, and EF.[51]

In other studies, GM–CSF delivery has been reported to result in significant angiogenesis within mouse models of acute MI.[52] These preclinical findings have been supported in clinical studies where subcutaneous delivery of GM–CSF has been demonstrated to result in collateral growth promotion in patients with coronary artery disease.[53] However, in these same clinical studies, GM–CSF treatment may also have caused atherosclerotic plaque rupture possibly due to its proartherogenic action through its

TABLE 1. Hemodynamic Parameters

Treatment	LVDd (mm)	LV SP (mm Hg)	LV EDP (mm Hg)	Tau (ms)
Sham	0.5 ± 0.04	124 ± 5	6 ± 2	20 ± 4
MI*	1 ± 0.04	109 ± 4	22 ± 4	25 ± 2
MI + anti-GM–CSF*	0.9 ± 0.05	104 ± 5	20 ± 2	22 ± 1

Data are mean ± SE.
Sham (n = 4–5), MI (n = 7–12), MI + anti-GM–CSF (n = 7–10).
*$P < 0.05$ versus sham.
LVDd, left ventricular end diastolic diameter; LV SP, left ventricular systolic pressure; LV EDP, left ventricular end diastolic pressure; Tau, relaxation time.

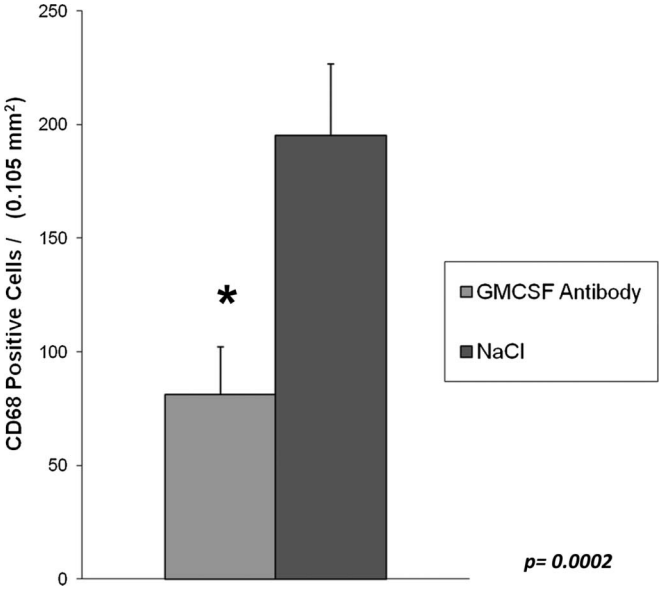

FIGURE 4. CD68 positive cells per HPF.

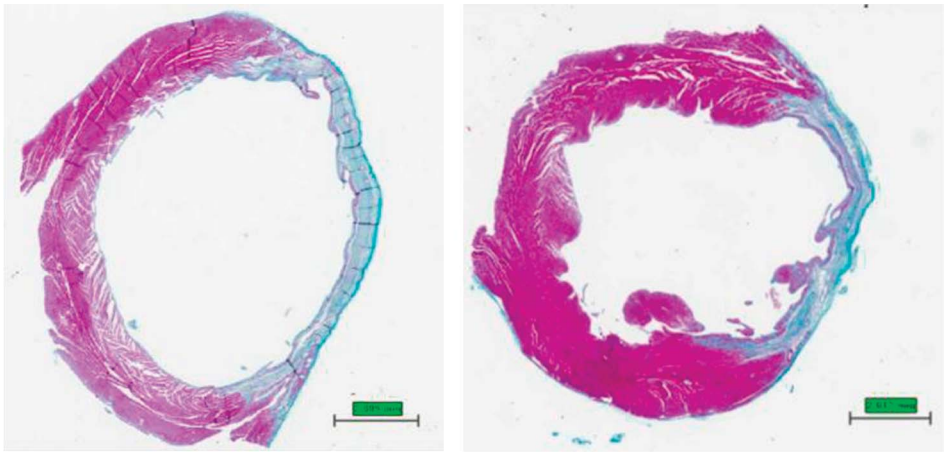

FIGURE 5. Representative trichrome staining of left ventricle cross sections from NaCl control (left) and anti-GM–CSF–treated (right) heart. Scale bars = 2.0 mm.

MCP-1 elevating effect.[16,53] To date, a number of clinical trials using GM–CSF or G-CSF have been stopped early due to safety concerns.[53,54] Both GM–CSF and G-CSF have been labeled as "Double-Edged Swords."[55] Although both of these compounds have been shown to be strong angiogenic, or arteriogenic factors, they also have robust proinflammatory and procoagulant effects.[56]

In this study, anti-GM–CSF–treated animals had significantly fewer activated tissue macrophages present in comparison to saline control animals. We did not discriminate whether the anti-GM–CSF was inhibiting migration of macrophages into the damaged myocardium or if the activity was to inhibit the activation of tissue macrophages. Nevertheless, significantly fewer CD68 positive (activated) macrophages were detected in the damaged myocardium and these anti-GM–CSF-treated animals had significant reductions in infarct size suggesting a more favorable myocardial remodeling process, postinfarction. Furthermore, anti-GM–CSF–treated animals demonstrated improvements in LV EF thus suggesting the anti-GM–CSF treatment was effective in mitigating a loss of LV function and decreasing the presence of inflammatory cells in the damaged myocardium. We did not detect any significant differences between anti-GM–CSF-treated animals and saline control animals with respect to microvascular elements in the damaged myocardium. These data suggest that inhibition of GM–CSF activity may be beneficial in the prevention or treatment of heart failure after MI.

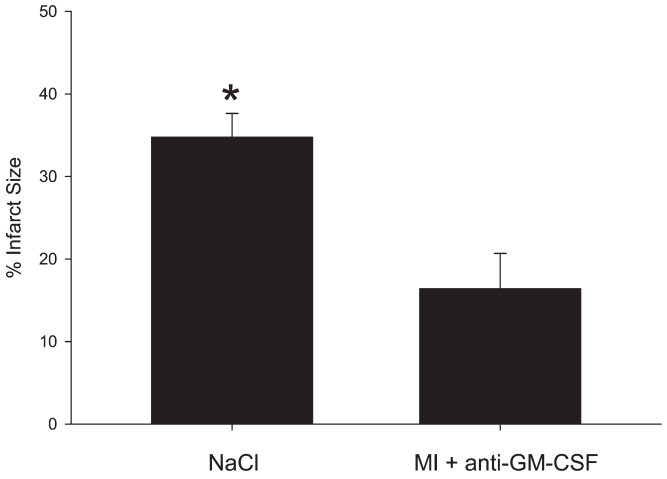

FIGURE 6. Morphometry analysis of NaCl-treated hearts (n = 5) and anti-GM–CSF–treated hearts (n = 5) using Aperio whole-slide scanned images and the ImageScope Software v10.0.36.1808. Data are mean ± SE. *$P < 0.01$.

REFERENCES

1. Braunwald E. Shattuck lecture—cardiovascular medicine at the turn of the millennium: triumphs, concerns, and opportunities. *N Engl J Med*. 1997; 337:1360–1369.
2. Weber KT, Pick R, Silver MA, et al. Fibrillar collagen and remodeling of dilated canine left ventricle. *Circulation*. 1990;82:1387–1401.
3. Volders PG, Willems IE, Cleutjens JP, et al. Interstitial collagen is increased in the non-infarcted human myocardium after myocardial infarction. *J Mol Cell Cardiol*. 1993;25:1317–1323.
4. Anderson KR, Sutton MG, Lie JT. Histopathological types of cardiac fibrosis in myocardial disease. *J Pathol*. 1979;128:79–85.
5. Anversa P, Olivetti G, Capasso JM. Cellular basis of ventricular remodeling after myocardial infarction. *Am J Cardiol*. 1991;68:7D–16D.
6. Olivetti G, Abbi R, Quaini F, et al. Apoptosis in the failing human heart. *N Engl J Med*. 1997;336:1131–1141.
7. Tan LB, Jalil JE, Pick R, et al. Cardiac myocyte necrosis induced by angiotensin II. *Circ Res*. 1991;69:1185–1195.
8. Weisman HF, Bush DE, Mannisi JA, et al. Global cardiac remodeling after acute myocardial infarction: a study in the rat model. *J Am Coll Cardiol*. 1985;5:1355–1362.
9. Torre-Amione G, Kapadia S, Benedict C, et al. Proinflammatory cytokine levels in patients with depressed left ventricular ejection fraction: a report from the Studies Of Left Ventricular Dysfunction (SOLVD). *J Am Coll Cardiol*. 1996;27:1201–1206.
10. Testa M, Yeh M, Lee P, et al. Circulating levels of cytokines and their endogenous modulators in patients with mild to severe congestive heart failure due to coronary artery disease or hypertension. *J Am Coll Cardiol*. 1996;28:964–971.
11. Ferrari R, Bachetti T, Confortini R, et al. Tumor necrosis factor soluble receptors in patients with various degrees of congestive heart failure. *Circulation*. 1995;92:1479–1486.
12. Deswal A, Petersen NJ, Feldman AM, et al. Cytokines and cytokine receptors in advanced heart failure: an analysis of the cytokine database from the Vesnarinone trial (VEST). *Circulation*. 2001;103:2055–2059.
13. Maekawa Y, Anzai T, Yoshikawa T, et al. Prognostic significance of peripheral monocytosis after reperfused acute myocardial infarction: a possible role for left ventricular remodeling. *J Am Coll Cardiol*. 2002; 39:241–246.
14. Hong YJ, Jeong MH, Ahn Y, et al. Relationship between peripheral monocytosis and nonrecovery of left ventricular function in patients with left ventricular dysfunction complicated with acute myocardial infarction. *Circ J*. 2007;71:1219–1224.

15. Gasson JC. Molecular physiology of granulocyte–macrophage colony-stimulating factor. *Blood*. 1991;77:1131–1145.
16. Tanimoto A, Murata Y, Wang KY, et al. Monocyte chemoattractant protein-1 expression is enhanced by granulocyte–macrophage colony-stimulating factor via Jak2-Stat5 signaling and inhibited by atorvastatin in human monocytic U937 cells. *J Biol Chem*. 2008;283:4643–4651.
17. Kohno Y, Tanimoto A, Cirathaworn C, et al. GM–CSF activates RhoA, integrin and MMP expression in human monocytic cells. *Pathol Int*. 2004 Sep;54:693–702.
18. Parissis JT, Adamopoulos S, Venetsanou KF, et al. Clinical and neurohormonal correlates of circulating granulocyte–macrophage colony-stimulating factor in severe heart failure secondary to ischemic or idiopathic dilated cardiomyopathy. *Am J Cardiol*. 2000;86:707–710, A9–A10.
19. Postiglione L, Montagnani S, Ladogana P, et al. Granulocyte macrophage-colony stimulating factor receptor expression on human cardiomyocytes from end-stage heart failure patients. *Eur J Heart Fail*. 2006;8:564–570.
20. Naito K, Anzai T, Sugano Y, et al. Differential effects of GM–CSF and G-CSF on infiltration of dendritic cells during early left ventricular remodeling after myocardial infarction. *J Immunol*. 2008;181:5691–5701.
21. Maekawa Y, Anzai T, Yoshikawa T, et al. Effect of granulocyte–macrophage colony-stimulating factor inducer on left ventricular remodeling after acute myocardial infarction. *J Am Coll Cardiol*. 2004; 44:1510–1520.
22. Raya TE, Gay RG, Aguirre M, et al. The importance of venodilatation in the prevention of left ventricular dilatation after chronic large myocardial infarction in rats: a comparison of captopril and hydralazine. *Circ Res*. 1989;64: 330–338.
23. Gaballa M, Raya TE, Goldman S. Large artery remodeling after myocardial infarction. *Am J Physiol*. 1995;268:H2092–H2103.
24. Raya TE, Gaballa M, Anderson P, et al. Left ventricular function and remodeling after myocardial infarction in aging rats. *Am J Physiol*. 1997; 273(pt 2):H2652–H2658.
25. Goldman S, Raya TE. Rat infarct model of myocardial infarction and heart failure. *J Card Fail* 1995;1:169–177.
26. Pennock GD, Raya TE, Bahl JJ, et al. Combination treatment with captopril and the thyroid hormone analog 3,5-diiodothyropropionic acid (DITPA): a new approach to improving left ventricular performance in heart failure. *Circulation*. 1993;88:1289–1298.
27. Gaballa MA, Goldman S.Ventricular remodeling in heart failure. *J Card Fail* 2002;6:S476–S485, 2002.
28. Frangogiannis NG, Smith CW, Entman ML. The inflammatory response in myocardial infarction. *Cardiovasc Res*. 2002;53:31–47.
29. Frangogiannis NG, Youker KA, Rossen RD, et al. Cytokines and the microcirculation in ischemia and reperfusion [Review]. *J Mol Cell Cardiol*. 1998;30:2567–2576.
30. Mehta JL, Li DY. Inflammation in ischemic heart disease: response to tissue injury or a pathogenetic villain? [Review] *Cardiovasc Res*. 1999;43: 291–299.
31. Buschmann IR, Hoefer IE, van Royen N, et al. GM-CSF: a strong arteriogenic factor acting by amplification of monocyte function. *Atherosclerosis*. 2001;159:343–356.
32. Coxon A, Tang T, Mayadas TN. Cytokine-activated endothelial cells delay neutrophil apoptosis in vitro and in vivo. A role for granulocyte/macrophage colony-stimulating factor. *J Exp Med*. 1999;190:923–934.
33. Frangogiannis NG. The mechanistic basis of infarct healing. *Antioxid Redox Signal*. 2006;8:1907–1939.
34. Murakami Y, Kurosaki K, Matsui K, et al. Serum MCP-1 and VEGF levels are not affected by inhibition of the renin–angiotensin system in patients with acute myocardial infarction. *Cardiovasc Drugs Ther*. 2003; 17:249–255.
35. de Lemos JA, Morrow DA, Sabatine MS, et al. Association between plasma levels of monocyte chemoattractant protein-1 and long-term clinical outcomes in patients with acute coronary syndromes. *Circulation*. 2003;107:690–695.
36. Parissis JT, Adamopoulos S, Venetsanou KF, et al. Serum profiles of C–C chemokines in acute myocardial infarction: possible implication in postinfarction left ventricular remodeling. *J Interferon Cytokine Res*. 2002;22:223–229.
37. Dewald O, Zymek P, Winkelmann K, et al. CCL2/monocyte chemoattractant protein-1 regulates inflammatory responses critical to healing myocardial infarcts *Circ Res*. 2005;96:881–889.
38. Hayashidani S, Tsutsui H, Shiomi T, et al. Anti-monocyte chemoattractant protein-1 gene therapy attenuates left ventricular remodeling and failure after experimental myocardial infarction. *Circulation*. 2003;108:2134–2140.
39. Simpson PJ, Todd RF III, Fantone JC, et al. Reduction of experimental canine myocardial reperfusion injury by a monoclonal antibody (anti-Mo1, anti-CD11b) that inhibits leukocyte adhesion. *J Clin Invest*. 1988 81:624–629.
40. Simpson PJ, Todd RF III, Mickelson JK, et al. Sustained limitation of myocardial reperfusion injury by a monoclonal antibody that alters leukocyte function. *Circulation*. 1990;81:226–237.
41. Cleutjens JP, Kandala JC, Guarda E, et al. Regulation of collagen degradation in the rat myocardium after infarction. *J Mol Cell Cardiol*. 1995;27:1281–1292.
42. Peterson JT, Li H, Dillon L, et al. Evolution of matrix metalloprotease and tissue inhibitor expression during heart failure progression in the infarcted rat. *Cardiovasc Res*. 2000;46:307–315.
43. Trueblood NA, Xie Z, Communal C, et al. Exaggerated left ventricular dilation and reduced collagen deposition after myocardial infarction in mice lacking osteopontin. *Circ Res*. 2001;88:1080–1087.
44. Whittaker P, Boughner DR, Kloner RA. Role of collagen in acute myocardial infarct expansion. *Circulation*. 1991;84:2123–2134.
45. Ducharme A, Frantz S, Aikawa M, et al. Targeted deletion of matrix metalloproteinase-9 attenuates left ventricular enlargement and collagen accumulation after experimental myocardial infarction. *J Clin Invest*. 2000;106:55–62.
46. Rohde LE, Ducharme A, Arroyo LH, et al. Matrix metalloproteinase inhibition attenuates early left ventricular enlargement after experimental myocardial infarction in mice. *Circulation*. 1999;99:3063–3070.
47. Wu L, Tanimoto A, Murata Y, et al. Induction of human matrix metalloproteinase-12 gene transcriptional activity by GM-CSF requires the AP-1 binding site in human U937 monocytic cells. *Biochem Biophys Res Commun*. 2001;285:300–307.
48. Kohno Y, Tanimoto A, Cirathaworn C, et al. GM-CSF activates RhoA, integrin and MMP expression in human monocytic cells. *Pathol Int*. 2004; 54:693–702.
49. Armitage JO. Emerging applications of recombinant human granulocyte–macrophage colony-stimulating factor. *Blood*. 1998;92:4491–4508.
50. Honkoop AH, Hoekman K, Wagstaff J, et al. Continuous infusion or subcutaneous injection of granulocyte–macrophage colony stimulating factor: increased efficacy and reduced toxicity when given subcutaneously. *Br J Cancer*. 1996;74:1132–1136.
51. Knoops S, Groeneveld ABJ, Kamp O, et al. Granulocyte–macrophage colony-stimulating factor (GM–CSF) decreases left ventricular function. An echocardiographic study in cancer patients. *Cytokine*. 2001;14:184–187.
52. Yeghiazarians Y, Khan M, Angeli FS, et al. Cytokine combination therapy with long-acting erythropoietin and granulocyte colony stimulating factor improves cardiac function but is not superior than monotherapy in a mouse model of acute myocardial infarction. *J Card Fail*. 2010;16: 669–678.
53. Zbinden S, Zbinden R, Meier P, et al. Safety and efficacy of subcutaneous-only granulocyte–macrophage colony-stimulating factor for collateral growth promotion in patients with coronary artery disease. *J Am Coll Cardiol* 2005;46:1636–1642.
54. Hill JM, Syed MA, Arai AE, et al. Outcomes and risks of granulocyte colony-stimulating factor in patients with coronary artery disease. *J Am Coll Cardiol*. 2005;46:1643–1648.
55. Wilson RF, Henry TD. Granulocyte colony-stimulating factor and granulocyte–macrophage colony-stimulating factor: double-edged swords. *J Am Coll Cardiol* 2005;46:1649–1650.
56. Anderlini P, Przepiorka D, Champlin R, et al. Biologic and clinical effects of granulocyte colony-stimulating factor in normal individuals. *Blood*. 1996;88:2819–2825.

